Accurate experimental (p, ρ, T) data of the $(CO_2 + O_2)$ binary system for the development of models for CCS processes

Daniel Lozano-Martín¹, Gerald U. Akubue^{1,2}, Alejandro Moreau¹, Dirk Tuma³, and César R. Chamorro¹.

¹ Grupo de Termodinámica y Calibración (TERMOCAL), Research Institute on Bioeconomy, Escuela de

Ingenierías Industriales, Universidad de Valladolid, Paseo del Cauce, 59, E-47011 Valladolid, Spain.

² National Centre for Energy Research and Development & Mechanical Engineering Department, University

of Nigeria, Nsukka, 410001 Enugu State, Nigeria

³ BAM Bundesanstalt für Materialforschung und -prüfung, D-12200 Berlin, Germany.

Abstract

The limited availability of accurate experimental data in wide ranges of pressure, temperature, and composition is the main constraining factor for the proper development and assessment of thermodynamic models and equations of state. In the particular case of carbon capture and storage (CCS) processes, there is a clear need for data sets related to the (carbon dioxide + oxygen) mixtures that this work aims to address. This work provides new experimental (p, ρ, T) data for three binary $(CO_2 + O_2)$ mixtures with mole fractions of oxygen $x(O_2) = (0.05, 0.10, \text{ and } 0.20) \text{ mol·mol·}^1$, in the temperature range T = (250 to 375) K and pressure range p = (0.5 to 13) MPa. The measurements were performed with a high-precision single-sinker densimeter with magnetic suspension coupling. The density data were obtained with estimated expanded relative uncertainties of 0.02 % for the highest densities, and up to 0.3 % for the lowest ones. The results were compared to the corresponding results calculated by the current reference equations of state for this kind of mixtures, namely the EOS-CG (combustion gases) and the GERG-2008 equation of state, respectively. The EOS-CG yields better estimations in density than the GERG-2008 equation of state. The results from the EOS-GC model show no systematic temperature dependence. For the GERG-2008 model, however, this criterion is significantly less fulfilled.

Keywords: carbon capture and storage (CCS); density of binary mixtures ($CO_2 + O_2$); gravimetric preparation; single-sinker densimeter; equation of state.

* Corresponding author e-mail: cescha@eii.uva.es. Tel.: +34 983423756. Fax: +34 983423363

1. Introduction

The design and operation of Carbon Capture and Storage (CCS) processes need reliable thermodynamic models able to accurately describe the behavior of the fluid mixtures of CO₂ with other gases [1][2]. Besides CO₂, the main components involved in those processes related to CCS technologies are N₂, O₂, Ar, H₂O, H₂, CO, H₂S, and SO₂. An approved thermodynamic model able to describe fluid mixtures of these components over an extended *p*,*T*-region is the GERG-2008 equation of state [3], which is based on a multifluid mixture model and explicit in the reduced Helmholtz free energy. However, this EoS was originally developed for natural gas mixtures and thus does not a priori guarantee a high accuracy for mixtures with a composition far from that of typical natural gas mixtures, such as CCS mixtures with perhaps no methane present in them at all, but with CO₂ as the main compound.

Some specific EoS have recently been developed for mixtures involved in CCS processes. Demetriades and Graham [4] proposed a pressure-explicit EoS for mixtures of CO₂ with small quantities (impurities) of N₂, O₂, and H₂. The range of validity of this model is for pressures up to 16 MPa and temperatures between 273 K and the critical temperature of CO₂. A recent research work [5] has proposed a specific model for the binary mixture (CO₂ + CO). Gernert and Span proposed an equation of state for the calculation of thermodynamic properties of humid gases, combustion gases, and CO₂-rich mixtures typical in CCS processes, the so-called EOS-CG (Equation of State for Combustion Gases and Combustion Gas-like Mixtures) [6]. This equation of state, with a functional structure similar to the GERG-2008, based on a multi-fluid mixture model explicit in the reduced Helmholtz free energy, has a wider range of validity in temperature and pressure, and more components are considered. The EOS-CG has been developed for 6 constituting pure components: CO₂, N₂, O₂, Ar, H₂O, and CO. Unfortunately, binary specific departure functions were developed (or, in some case, taken from the GERG-2008 EoS) for only some of the 15 resulting binary mixtures, those for which sufficiently accurate experimental data were available. As for the binary mixture (carbon dioxide + oxygen), no departure function has yet been developed due to limited experimental data.

High-accuracy density data are of great relevance for the development of reliable equations of state for CCS processes [7]. In this work, accurate density measurements for three binary mixtures of carbon dioxide with oxygen (nominal amount-of-substance fraction $x(O_2) = 0.05$, 0.10, 0.20) are presented. Measurements were

performed at temperatures between (250 and 375) K and pressures up to 13 MPa, using a single-sinker densimeter with magnetic suspension coupling, which is one of the state-of-the-art methods for density determination over wide ranges of temperature and pressure. In order to achieve the highest accuracy in composition, the binary mixtures for this investigation were prepared gravimetrically according to the ISO 6142-1 [8], a method that qualifies for the production of reference materials. The experimental results are compared with the calculations by both the GERG-2008 equation of state and the EOS-CG, and also with the limited experimental data available in the literature.

2. Experimental

2.1. Mixture preparation

Three $(CO_2 + O_2)$ binary mixtures were prepared at the Federal Institute for Materials Research and Testing (Bundesanstalt für Materialforschung und -prüfung, BAM) in Berlin, Germany, following the recommendations given in the standard ISO 6142-1 [8].

Purity, supplier, molar mass, and critical parameters of the pure compounds (obtained from the reference equations of state for carbon dioxide [9] and oxygen [10]) are given in Table 1. Table 2 shows the gravimetric composition and its corresponding absolute expanded uncertainty (k = 2) of the three mixtures. Carbon dioxide and oxygen were used without further purification, but information on impurities from the specification was considered in the preparation of the mixture.

Prior to the preparation, the mass portions of the constituting compounds had to be calculated. The phase boundary was calculated applying the GERG-2008 EoS, and the gas portions were adapted in such a way that a homogeneous gas phase would be inside the cylinder at room temperature.

The preparation of the mixtures (BAM reference gas mixture G 033) consisted of two consecutive steps in which the pure compound was transferred. First, pure carbon dioxide was introduced into the evacuated recipient cylinder. The carbon dioxide was taken from the liquid phase, which required an upside-down mounting of the feed cylinder. Heating of the feed cylinder was administered during the transfer to enlarge the pressure difference between the two cylinders. The oxygen was introduced in the second step from a feed cylinder that had sufficient internal pressure to ensure the transfer of the required mass portion. During each filling step, the recipient cylinder stood on the platform of an electronic comparator balance (Sartorius

LA 34000P-0CE, Sartorius AG, Göttingen, Germany, weighing range: 34 kg, readability: 0.1 g) to monitor the feed stream. The exact mass of the gas added was determined after each filling step using a high-precision mechanical balance (Voland model HCE 25, Voland Corp., New Rochelle NY, USA, weighing range: 25 kg, readability: 2.5 mg).

The following gas portions were determined that resulted in the final pressures:

Cylinder 1007-180626 ($x(O_2) = 0.05$): 1088.762 g CO₂ 41.946 g O₂ p = 5.8 MPa Cylinder 1008-180626 ($x(O_2) = 0.10$): 1137.833 g CO₂ 91.775 g O₂ p = 6.4 MPa Cylinder 9085-180116 ($x(O_2) = 0.20$): 1073.480 g CO₂ 195.014 g O₂ p = 6.8 MPa

After the filling, the three mixtures were homogenized by subsequent heating and rolling for approximately 8 hours each.

Prior to density determination, the cylinders were validated at BAM by gas chromatography (GC) on a multichannel process analyzer (Siemens MAXUM II, Siemens AG, Karlsruhe, Germany). Details of configuration and operation are given in a previous paper [11]. The matrix compound CO₂ was not analyzed for these mixtures, as the CO₂ content is outside the operational range of the GC. The bracketing method outlined in ISO 12963 was applied for validation [12]. The calibration mixtures were prepared by the gravimetric method using the same procedures as for the research samples. Any interdependence between both calibration gases and the research samples was thus avoided. The results of the GC analysis and the corresponding (gravimetric) composition of the binary mixtures used for validation can be found in Table 3. The deviations between gravimetric realization and GC analyses were low enough to pass the criteria for certification.

2.2. Equipment description

The (p, ρ, T) data were measured using a single-sinker magnetic suspension densimeter (SSMSD) especially designed for density measurements of pure gases and gaseous mixtures. Details of the equipment and measurement procedure have been previously described by Chamorro et al. [13], Mondéjar et al. [14], and Lozano-Martín et al. [15]. The measuring method, originally developed by Brachthäuser et al. [16] and improved by Klimeck et al. [17], operates on the Archimedes' principle. A magnetic suspension coupling system allows the determination of the buoyancy force on a sinker immersed in the gas so that accurate

density measurements of fluids over wide temperature and pressure ranges can be obtained. The sinker used in this work was cylindrical and made of monocrystalline silicon with a mass of 61.59181 ± 0.00016 g and a volume of 26.444 ± 0.003 cm³ (k = 2), measured at T = 293.05 K and p = 1.01134 bar, and determined at the Mass Division of the Spanish National Metrology Institute (Centro Español de Metrología, CEM). The magnetic coupling is formed by an electromagnet hanging from the lower hook of an analytical balance (Mettler Toledo XPE205DR, Mettler Toledo GmbH, Gießen, Germany, weighing range: 81 g, readability: 0.01 mg, extended weighing range: 220 g) and a permanent magnet inside the measuring cell. The permanent magnet is fixed to a sinker support, which allows the sinker to be coupled and decoupled from the balance. The magnetic coupling has two different positions: the zero position (ZP) and the measuring position (MP). A load compensation system consists of two calibrated masses, one made of tantalum and the other of titanium, which can be put on the upper pan of the balance. Both masses have approximately the same volume (4.9 cm³) and the mass difference between both is similar to the mass of the sinker. This characteristic system and the differential nature of the measurement procedure allow the balance to operate near its zero point and to perform a periodic calibration of the balance, free from the air buoyancy corrections. The two masses were provided by Rubotherm GmbH, Bochum, Germany, and their individual mass and volume were also accurately determined at the Mass Division of the CEM.

The temperature inside the measuring cell is determined by means of two platinum resistance thermometers (S1059PJ5X6, Minco Products, Inc., Minneapolis MN, USA). A very accurate monitoring and measurement of temperature is achieved using an AC comparator resistance bridge (F700, Automatic Systems Laboratories, Redhill, England) connected to the Pt thermometers and a reference resistance. The pressure inside the cell is recorded by two pressure transducers which cover different pressure ranges: a Paroscientific 2500A-101 for pressures from (0 to 3) MPa and a Paroscientific 43KR-HHT-101 (Paroscientific Inc., Redmond WA, USA) for pressures up to 20 MPa.

2.3. Density measurement procedure

A detailed description of the measurement procedure in SSMSD is presented by Mondéjar et al. [14] and Lozano-Martín et al. [15] for our equipment; and by McLinden [18] and Richter et al. [19] for general aspects. Basically, the density of the fluid can be calculated from Eq. (1):

$$\rho_{\text{fluid}} = \frac{m_{\text{so}} - m_{\text{sf}}}{V_{\text{s}}(T, p)} \tag{1}$$

where the difference between the result of weighing the sinker in vacuum m_{s0} and the result of weighing the sinker in the pressurized fluid m_{sf} is related to the buoyancy force exerted on the sinker which is determined using a high-precision microbalance. V_s (T, p) is the volume of the sinker immersed in the fluid, whose dependence on temperature and pressure is accurately known [14].

The measurement procedure involves obtaining the buoyancy force by subtracting the reading of the balance in two different positions of the magnetic coupling, namely the zero position (ZP) and the measuring position (MP). In the ZP the magnetic coupling attracts the permanent magnet, but the sinker is not lifted and continues to rest on the bottom of the cell. In the MP, the magnetic coupling attracts the permanent magnet a little more strongly, so the sinker is lifted. Simultaneously, the load compensation system places the tantalum mass on the upper pan of the balance when the magnetic coupling is in the ZP, and it places the titanium mass when the magnetic coupling is in the MP. The differential nature of the measuring method cancels the weights of the permanent magnet, the electromagnet, the hook and sinker support, and their corresponding buoyancy forces. The air buoyancy on the titanium and tantalum compensation loads is approximately equal, as both loads have the same volume, and their difference is also cancelled. To achieve maximum accuracy, the calibration of the balance and the correction for the force transmission error (FTE) [20] must be considered. The FTE arises from the different perturbations of the magnetic materials, the external magnetic fields, and the magnetic behavior of the fluid being measured to the force transmitted through the magnetic coupling system. So, the final expression to obtain the experimental density is given by the more specific equation (2):

$$\rho_{\rm fluid} = \frac{\phi_0 m_{\rm s} + (m_{\rm Ti} - m_{\rm Ta}) - (W_{\rm ZP} - W_{\rm MP})/\alpha}{V_{\rm s}(T,p)} \frac{1}{\phi_0} + \frac{\varepsilon_\rho}{\phi_0} \frac{\chi_{\rm s}}{\chi_{\rm so}} \left(\frac{\rho_{\rm s}}{\rho_0} - \frac{\rho_{\rm fluid}}{\rho_0}\right) \rho_{\rm fluid} \tag{2}$$

Equation (2) results from the applied method and thus should be explained in detail. The experimental density of the fluid is written as the sum of two terms. The first term stands for the density of the fluid if

only the correction for the apparatus-specific effect of the FTE is considered. The second term of the sum corrects the experimental density considering the effect on the magnetic coupling due to the individual magnetic susceptibility of the fluid being measured, the fluid-specific effect of the FTE.

Regarding the first term of the sum in equation (2), m_s , m_{Ti} , and m_{Ta} represent the masses of the silicon sinker and the titanium and tantalum compensation masses. ($W_{ZP} - W_{MP}$) is the difference between the balance readings when the magnetic coupling is in the ZP and in the MP. $V_S(T, p)$ is the volume of the sinker at the experimental temperature and pressure. α and Φ_0 are the balance calibration factor and the coefficient for the correction due to the apparatus-specific effect of the FTE (coupling factor).

The balance calibration factor α can easily be obtained by an independent calibration, free from the air buoyancy effect, using the two compensation masses. While the magnetic coupling is in the zero position (ZP), two measurements are recorded, one with the titanium mass on the balance pan ($W_{\text{ZP,Ti}}$), and the other with the tantalum mass ($W_{\text{ZP,Ta}}$). Subtracting one from the other gives the value of α :

$$\alpha = \frac{W_{\text{ZP,Ta}} - W_{\text{ZP,Ti}}}{(m_{\text{Ta}} - m_{\text{Ti}})} \tag{3}$$

The balance calibration factor is measured directly before and after every single measurement point during the measurement campaign.

The term Φ_0 accounts for the apparatus-specific effect of the FTE in the reading of the balance. It can be obtained by weighing the sinker in vacuum:

$$\Phi_0 = \frac{-(m_{\text{Ti}} - m_{\text{Ta}}) + (W_{\text{ZP,vacuum}} - W_{\text{MP,vacuum}}) / \alpha}{m_{\text{s}}}$$
(4)

The apparatus-specific effect Φ_0 is temperature-dependent and very sensitive to changes in the alignment of the electromagnet with respect to the permanent magnet, so it is experimentally determined at the end of every single isotherm to guarantee the highest accuracy of the measurement.

The second term on the right-hand side of equation (2) corrects the experimental density with the effect on the magnetic coupling due to the magnetic susceptibility of the fluid being measured (fluid-specific effect of the FTE). It should be pointed out that an approximate initial value of ρ_{fluid} must be introduced to obtain this second term. The value of density which results from the first term of the right-hand side of that same equation is a good approximation for this purpose. The quantities $\chi_{s0} = 10^{-8} \text{ m}^3 \cdot \text{kg}^{-1}$ and $\rho_0 = 1000 \text{ kg} \cdot \text{m}^{-3}$, which appear in equation (2), are reducing constants for the mass-based magnetic susceptibility of the fluid χ_s , the density of the fluid ρ_{fluid} , and the density of the sinker ρ_s . The term ε_ρ , called the 'apparatus-specific constant of the fluid-specific effect', is specific for any particular SSMSD and was calculated for our equipment from density measurements on pure oxygen over a wide range of temperatures and pressures [15]. The obtained value for ε_ρ , as a function of temperature and density, is given by equation (5):

$$\varepsilon_{\rho}(T,\rho) = 8.822 \cdot 10^{-5} + 4.698 \cdot 10^{-8} \cdot (T/K - 293.15) - 3.015 \cdot 10^{-8} \cdot \rho/(kg \cdot m^{-3})$$
 (5)

The mass-based magnetic susceptibilities χ_s for the three (CO₂ + O₂) binary mixtures studied in this work were estimated using the additive law proposed by Bitter [21]:

$$\chi_{s}(T) = \chi_{CO_{2}} \cdot \frac{M_{CO_{2}}}{M_{\text{mixture}}} \cdot \chi_{s,CO_{2}} + \chi_{O_{2}} \cdot \frac{M_{O_{2}}}{M_{\text{mixture}}} \cdot \chi_{s,O_{2}}(T)$$
(6)

where x_{CO2} and x_{O2} are the mole fractions of the components of the mixture and M_{CO2} , M_{O2} , and M_{mixture} are the molar mass of the components of the mixture and of the mixture itself. The mass-based magnetic susceptibility of carbon dioxide has a weak value of $\chi_{s,\text{CO2}} = -0.6 \cdot 10^{-8} \text{ m}^3 \cdot \text{kg}^{-1}$ [22], with no temperature dependence, as is characteristic for diamagnetic fluids. The molar magnetic susceptibility of molecular oxygen at the reference state, T = 293.15 K, p = 0 MPa, and zero frequency, is taken as $\chi_{\text{M00}} = (42.92 \pm 0.06) \cdot 10^{-9} \text{ m}^3 \cdot \text{mol}^{-1}$, a value measured by May et al. [23] and in close accordance with the ab initio calculation of Minaev [24]. With $M_{\text{O2}} = 31.9988 \text{ g} \cdot \text{mol}^{-1}$ taken as the molar mass of oxygen, this gives a mass-based magnetic susceptibility of oxygen at the reference state of $\chi_{00} = 1.341 \cdot 10^{-6} \text{ m}^3 \cdot \text{kg}^{-1}$. Additionally, the dependence of the magnetic susceptibility of strong paramagnetic fluids, such as oxygen, with temperature should not be neglected [23]. The Curie law, which states that the magnetic susceptibility is proportional to 1/T, has been used to account for this temperature dependence:

$$\chi_{s,O_2}(T) = \chi_{00} \frac{293.15 \,\mathrm{K}}{T} \tag{7}$$

Even though the magnetic susceptibility of pure oxygen may also have a weak dependence with density [23], resulting in a decrease in the magnetic susceptibility with increasing density; this effect is not to be considered here, as it is already taken into account with the density dependence of ε_{ρ} reflected in equation (5) [15].

2.4. Experimental procedure

Experimental density data for the three ($CO_2 + O_2$) binary mixtures ($x(O_2) = 0.05$, 0.10 and 0.20) were obtained at temperatures of (250, 260, 275, 293.15, 300, 325, 350, and 375) K and pressures up to 13 MPa. In the course of a measurement campaign for each isotherm, the pressure was reduced in 1 MPa steps, starting from the highest measured pressure down to 1 MPa. Figure 1 illustrates the recorded data as coordinates in a p, T-diagram together with the saturation curve for the mixture calculated with the EOS-CG [6]. The p, T-range of applicability of the EOS-CG and the main area of interest for CCS applications are also represented in the three plots of Figure 1.

Thirty repeated measurements are recorded for each single (p, ρ, T) point and the last ten values are used to obtain the mean value. The balance calibration factor α is obtained right before and after every single point, and the apparatus-specific effect Φ_0 is determined at the end of every single isotherm.

Sorption effects inside the measuring cell may be responsible for errors of up to 0.1 % in density [19]. In order to minimize this effect, the measuring cell is evacuated and flushed several times with fresh mixture before each isotherm is measured, as recommended by Richter and Kleinrahm [19]. The residence time of the mixture in the cell is never longer than 40 hours. Specific sorption tests for this particular mixture were performed in the same way as they were done in previous investigations [11], [25]–[35]. Continuous density measurements on the same state point were recorded over 48 hours. These results showed that the difference observed in the trend of the relative deviation in density from the GERG-2008 EoS between the first and the last measurement is one order of magnitude lower than the density uncertainty. A measurement with

fresh mixture executed immediately afterwards, for the same temperature and pressure, also repeated the density value with a deviation of one order of magnitude lower than the density uncertainty. Therefore, residual errors due to sorption effects are not appreciable with the experimental technique, and it should be considered that they are already included in the measurement uncertainty of the density and in the uncertainty of the composition.

The performance of the experimental technique and the measurement method was checked before and after the measurements of the three ($CO_2 + O_2$) mixtures, using nitrogen as the reference fluid over the entire operational range of the apparatus. These results were compared to the densities calculated from the reference equation of state for nitrogen by Span et al. [36]. The relative deviations of the 113 experimental densities of nitrogen, measured over seven different isotherms from 240 K to 350 K and for pressures up to 20 MPa, agreed with those calculated from the reference equation of state as the relative deviations remain within a ± 0.02 % band, with an absolute average deviation (AAD) of 0.014 %.

2.5. Uncertainty of the measurements

A detailed analysis of the uncertainties of the measurements involved in this experimental procedure was reported in previous works [14][15]. The expanded uncertainty in temperature (k = 2) is less than 4 mK. The pressure uncertainty depends on the range and is given by Eq. (8) and Eq. (9) for the (3 to 20) MPa and (0 to 3) MPa transducers, respectively. The expanded uncertainty (k = 2) in pressure is in both cases less than 0.005 MPa.

$$U(p)/MPa = 75 \cdot 10^{-6} \cdot p/MPa + 3.5 \cdot 10^{-3}$$
(8)

$$U(p)/\text{MPa} = 60 \cdot 10^{-6} \cdot p/\text{MPa} + 1.7 \cdot 10^{-3}$$
(9)

The uncertainty of density data for the three $(CO_2 + O_2)$ binary mixtures, corrected by both the apparatusspecific and the fluid-specific FTE effects, $U(\rho_{\text{fluid}})$, is evaluated directly by applying the law of propagation of uncertainty, according to the Guide to the Expression of Uncertainty in Measurement (GUM) [37], to equation (2). The estimation of the uncertainty was thoroughly explained in a previous paper [15] and can be given by the expression:

$$U(\rho)/\text{kg} \cdot \text{m}^{-3} = 2.5 \cdot 10^4 \cdot \chi_s/\text{m}^3 \cdot \text{kg}^{-1} + 1.1 \cdot 10^{-4} \cdot \rho/\text{kg} \cdot \text{m}^{-3} + 2.3 \cdot 10^{-2}$$
(10)

To calculate the overall expanded uncertainty in density $U_T(\rho)$ (k=2), the uncertainties of density, temperature, pressure, and composition of the mixture must be included, as expressed in Eq. (11):

$$U_{\mathrm{T}}(\rho) = 2 \cdot \left[u(\rho)^{2} + \left(\left(\frac{\partial \rho}{\partial p} \right)_{T,x} \cdot u(p) \right)^{2} + \left(\left(\frac{\partial \rho}{\partial T} \right)_{p,x} \cdot u(T) \right)^{2} + \sum_{i} \left(\left(\frac{\partial \rho}{\partial x_{i}} \right)_{T,p,x_{j} \neq x_{i}} \cdot u(x_{i}) \right)^{2} \right]^{0.5}$$
(11)

where p is the pressure, T is the temperature, and x_i is the amount-of-substance (mole) fraction of each component in the mixture. Partial derivatives were calculated from the GERG-2008 EoS using the REFPROP software [38].

Table 4 displays a summary of the uncertainty contributions of density, temperature, pressure, and composition to the overall uncertainty in density for the three studied $(CO_2 + O_2)$ binary mixtures.

3. Experimental results

Tables 5, 6, and 7 show the 162 experimental (p, ρ, T) data measured for the three $(CO_2 + O_2)$ binary mixtures. The temperature, pressure, and density of each measured point were calculated as the arithmetic mean of the last ten consecutive measurements of a series of thirty. Tables 5, 6, and 7 also show the expanded uncertainty in density $U(\rho_{exp})$ (k = 2), calculated by Eq. (10) and expressed in absolute density units and as a percentage of the measured density.

The experimental data were compared to the corresponding densities calculated from the GERG-2008 and the EOS-CG equations of state, using the REFPROP [38] and TREND 4.0 [39] software (with the original, short EoS used in the GERG model for pure fluids, instead of the more precise and more complex reference EoS for pure fluids used in REFPROP by default). The relative deviations of the experimental densities from these EoS are included in Tables 5, 6, and 7 and are shown in Figures 2, 3, and 4.

It is worth mentioning that the densities of the experimental points recorded in this work range from $\rho = 9.843 \text{ kg} \cdot \text{m}^{-3}$ (T = 260 K, p = 0.5 MPa, $x(O_2) = 0.20$) to $\rho = 478.56 \text{ kg} \cdot \text{m}^{-3}$ (T = 300 K, p = 12.3 MPa, $x(O_2) = 0.20$).

It is also worth pointing out the relevance of the correction due to the fluid-specific effect of the FTE, which can be applied from the estimation of the apparatus-specific constant ε_{ρ} of the fluid-specific effect in a previous work [15]. This correction is represented by the second term of the right-hand side of Eq. (2), and should be considered for any mixture with a high content of any paramagnetic fluid, such as oxygen, and increases with the density of the measured fluid. The correction due to the fluid-specific effect in the mixtures measured in this work can be as high as 1.313 kg·m⁻³ in absolute value (0.28 % relative value) at the high density of $\rho = 494.505$ kg·m⁻³, or 0.47 % in relative values (0.049 kg·m⁻³ absolute value) at the lowest density of $\rho = 10.322$ kg·m⁻³. In both cases, this applies to the mixture with the higher oxygen content (0.80 CO₂ + 0.20 O₂) at T = 300 K and T = 250 K, respectively.

4. Discussion of the results

Figure 2 shows the relative deviations of the experimentally determined density data of the $(0.95 \text{ CO}_2 + 0.05 \text{ O}_2)$ mixture from the corresponding density data calculated by the GERG-2008 (a) and the EOS-CG (b) models. In the same way, Figures 3 and 4 show the deviations for the $(0.90 \text{ CO}_2 + 0.10 \text{ O}_2)$ mixture and the $(0.80 \text{ CO}_2 + 0.20 \text{ O}_2)$ mixture, respectively.

Both equations of state claim an uncertainty in density of 1.0 % for mixtures of CO₂ and O₂, over the temperature range from (250 to 450) K and at pressures up to 35 MPa. The estimated uncertainty of the experimental density data ranges from 0.017 %, for T = 300 K, p = 12.3 MPa ($\rho = 478.56$ kg·m⁻³), to 0.211 % for T = 375 K, p = 1.0 MPa ($\rho = 13.550$ kg·m⁻³), in both cases for the (0.80 CO₂ + 0.20 O₂) mixture. A slightly bigger relative uncertainty of 0.3 % can be found in two single points, for the (0.80 CO₂ + 0.20 O₂) mixture, at T = 250 K and 260 K. This is because these are the only two points that have been measured at the lowest pressure of p = 0.5 MPa and show the lowest densities within this study ($\rho = 9.843$ kg·m⁻³ and $\rho = 10.322$ kg·m⁻³). Thus, for most of the measurements, the experimental expanded (k = 2) uncertainty is two orders of magnitude lower than the stated uncertainty of both equation-of-state models; and, even at the lowest experimental density, the estimated experimental uncertainty is still three times lower.

The relative deviations of the experimental density data from those calculated by GERG-2008 for the (0.95 CO₂ + 0.05 O₂) mixture (Figure 2 (a)) remain within the claimed uncertainty of the equation of state for all the 45 experimental points except for three. These three points correspond to the highest measured pressure of each of the three lowest temperatures measured (T = 275 K and p = 4.0 MPa; T = 293.15 K and p = 5.0MPa; and T = 300 K and p = 6.0 MPa). The relative deviations for these three points are between 1.2 % and 1.5 %. The deviations from this equation-of-state model increase as the oxygen content in the mixture increases. For the (0.90 CO₂ + 0.10 O₂) mixture, 10 of the 47 experimental points already deviate by more than the claimed uncertainty of the GERG-2008 EoS (Figure 3 (a)). These points belong to the highest pressures measured at temperatures of 275 K, 293.15 K, 300 K and 325 K. The relative deviations can become as high as 4.4 %. For the (0.80 CO₂ + 0.20 O₂) mixture, 31 of the 70 measured points deviate by more than the claimed uncertainty of the GERG-2008 EoS (Figure 4 (a)). This behavior depends on the temperature, as the points are located outside the margin for pressures over 2 MPa at T = 250 and 260 K, over 3 MPa at T = 275 K, over 4 MPa at T = 293.15 and 300 K, over 6 MPa at T = 325 K, over 9 MP = 350 K, and over 12 MPa at T = 375 K. The relative deviations can amount to as much as 6.6 %. In this mixture, we observe a non-monotonous run with increasing pressures. At T = 300 K, the relative deviation goes through a distinct maximum at approximately 10 MPa. Generally speaking, the GERG-2008 EoS can fit the experimental data within its claimed uncertainty only for the mixture with a lower oxygen content. The deviations visibly increase when the oxygen content increases, , this being particularly pronounced at lower temperatures and higher pressures. Furthermore, the deviations always have a positive value, i.e., the GERG-2008 underestimates the density of (CO₂ + O₂) mixtures, notably for mixtures with a high oxygen content, at high pressures and low temperatures.

The relative deviations of the experimental density data from those calculated by the other model, the EOS-CG (Figures 2 (b), 3 (b) and 4 (b)), for all the 162 experimental points, remain within the claimed uncertainty of the equation of state, except for three points, namely at $(x(O_2) = 0.10, T = 293.15 \text{ K}, p = 6.0 \text{ MPa})$, $(x(O_2) = 0.20, T = 300 \text{ K}, p = 11.0 \text{ MPa})$, and $(x(O_2) = 0.20, T = 300 \text{ K}, p = 12.2 \text{ MPa})$, where the relative deviation increases up to 1.2 %, -2.0 % and -3.2 %, respectively.

Table 8 presents the statistical parameters of the relative deviation of the experimental data from the corresponding densities calculated by the GERG-2008 and the EOS-CG model. The absolute average

deviation (AAD) of the experimental data from the densities calculated by the GERG-2008 EoS is of 0.29 % for the $(0.95 \text{ CO}_2 + 0.05 \text{ O}_2)$ mixture, 0.69 % for the $(0.90 \text{ CO}_2 + 0.10 \text{ O}_2)$ mixture, and 1.30 % for the $(0.80 \text{ CO}_2 + 0.20 \text{ O}_2)$ mixture. The corresponding AAD of the experimental data from the densities calculated by the EOS-CG model are 0.08 %, 0.15 %, and 0.22 %. For the three mixtures investigated in this study, all the statistical parameters that have been evaluated from the data processing are smaller for the EOS-CG model than the corresponding parameters for the GERG-2008 model.

The availability of data for $(CO_2 + O_2)$ mixtures in the literature is limited to oxygen contents below $x(O_2) = 0.15$ [40][41][42][43]. The statistical parameters of the relative deviation of these experimental data from the results of the two equation-of-state models are also given in Table 8.

5. Conclusions

New (p, ρ, T) high-precision experimental data for three binary mixtures of carbon dioxide and oxygen, with nominal compositions of $(0.95 \text{ CO}_2 + 0.05 \text{ O}_2)$, $(0.90 \text{ CO}_2 + 0.10 \text{ O}_2)$, and $(0.80 \text{ CO}_2 + 0.20 \text{ O}_2)$ at temperatures between (250 and 375) K and pressures up to 13 MPa, are reported. The experimental device used was a single-sinker densimeter with magnetic suspension coupling. The mixtures were prepared gravimetrically, which qualifies them as metrologically traceable reference mixtures.

The new experimental data were compared to the corresponding densities calculated by two equation-of-state models, the EOS-CG, which is specifically designed for combustion gases, and the GERG-2008, which is the established approach for working with natural gases. Both models claim an uncertainty margin of 1 % for the p, T-range investigated. The EOS-CG shows a good performance for the compositions investigated; the relative deviations in density were found to remain within the uncertainty margin of 1 % for almost all the data. The corresponding results from processing the GERG-2008, however, do not reach the same level as the results from the EOS-CG. The processed data show a significant deviation to positive values that becomes more pronounced towards lower temperatures, higher pressures, and higher oxygen contents. The deviation might be as high as about 7 % at 300 K and 10 MPa at $x(O_2) = 0.20$. It seems that the underlying basis still needs further input and these results might direct attention to mixtures with oxygen. Since the investigation of mixtures with a significant amount of oxygen is also a challenge from the point of view of safety, appropriate measures are required.

Acknowledgments

The authors wish to thank the Ministerio de Economía, Industria y Competitividad for their support through the project ENE2017-88474-R and the Junta de Castilla y León project VA280P18. The second author is grateful to the members of his affiliation group and program Erasmus + KA107-36589 ICM-UVa.

References

- [1] Li H, Jakobsen JP, Wilhelmsen Ø, Yan J. PVTxy properties of CO₂ mixtures relevant for CO₂ capture, transport and storage: Review of available experimental data and theoretical models. Appl Energy 2011;88(11):3567–79. https://doi.org/10.1016/j.apenergy.2011.03.052.
- [2] Munkejord ST, Hammer M, Løvseth SW. CO₂ transport: Data and models A review. Appl Energy 2016;169:499-523. https://doi.org/10.1016/j.apenergy.2016.01.100.
- [3] Kunz O, Wagner W. The GERG-2008 wide-range equation of state for natural gases and other mixtures: an expansion of GERG-2004. J Chem Eng Data 2012;57(11):3032–91. https://doi.org/10.1021/je300655b.
- [4] Demetriades TA, Graham RS. A new equation of state for CCS pipeline transport: Calibration of mixing rules for binary mixtures of CO₂ with N₂, O₂ and H₂. J Chem Thermodyn 2016;93:294–304. https://doi.org/10.1016/j.jct.2015.07.045.
- [5] Souza LFS, Herrig S, Span R, Trusler JPM. Experimental density and an improved Helmholtz-energy-explicit mixture model for (CO₂ + CO). Appl Energy 2019;251:113398. https://doi.org/10.1016/j.apenergy.2019.113398.
- [6] Gernert J, Span R. EOS-CG: A Helmholtz energy mixture model for humid gases and CCS mixtures.

 J Chem Thermodyn 2016;93:274–93. https://doi.org/10.1016/j.jct.2015.05.015.
- [7] Li H, Dong B, Yu Z, Yan J, Zhu K. Thermo-physical properties of CO₂ mixtures and their impacts on CO₂ capture, transport and storage: Progress since 2011. Appl Energy 2019;255:113789. https://doi.org/10.1016/j.apenergy.2019.113789.
- [8] ISO 6142-1. Gas Analysis preparation of calibration gas mixtures Part 1: gravimetric method for Class I mixtures. Geneva: International Organization for Standardization; 2015.

- [9] Span R, Wagner W. A new equation of state for carbon dioxide covering the fluid region from the triple-point temperature to 1100 K at pressures up to 800 MPa. J Phys Chem Ref Data 1996;25(6):1509–96. https://doi.org/10.1063/1.555991.
- [10] Schmidt R, Wagner W. A new form of the equation of state for pure substances and its application to oxygen. Fluid Phase Equilib 1985;19(3):175–200. https://doi.org/10.1016/0378-3812(85)87016-3.
- [11] Hernández-Gómez R, Tuma D, Villamañán R, Chamorro CR. Accurate experimental (*p*, *ρ*, *T*) data and virial coefficients for the (methane and helium) binary system. J Chem Thermodyn 2016;101:168–79. https://doi.org/10.1016/j.jct.2016.05.024.
- [12] ISO 12963. Gas analysis Comparison methods for the determination of the composition of gas mixtures based on one- and two-point calibration. Geneva: International Organization for Standardization; 2017.
- [13] Chamorro CR, Segovia JJ, Martín MC, Villamañán MA, Estela-Uribe JF, Trusler JPM. Measurement of the (pressure, density, temperature) relation of two (methane + nitrogen) gas mixtures at temperatures between 240 and 400 K and pressures up to 20 MPa using an accurate single-sinker densimeter. J Chem Thermodyn 2006;38(7):916–22. https://doi.org/10.1016/j.jct.2005.10.004.
- [14] Mondéjar ME, Segovia JJ, Chamorro CR. Improvement of the measurement uncertainty of a high accuracy single sinker densimeter via setup modifications based on a state point uncertainty analysis.

 Measurement 2011;44(9):1768–80. https://doi.org/10.1016/j.measurement.2011.07.012.
- [15] Lozano-Martín D, Mondéjar ME, Segovia JJ. Determination of the force transmission error in a single-sinker magnetic suspension densimeter due to the fluid-specific effect and its correction for use with gas mixtures containing oxygen. Measurement 2020;151:107176. https://doi.org/10.1016/j.measurement.2019.107176.
- [16] Brachthäuser K, Kleinrahm R, Lösch HW, Wagner W. Entwicklung eines neuen Dichtemeßverfahrens und Aufbau einer Hochtemperatur-Hochdruck-Dichtemeßanlage, Fortschr. Ber. VDI, Series 8, no. 173. Germany: VDI-Verlag. Düsseldorf; 1993.
- [17] Klimeck J, Kleinrahm R, Wagner W. An accurate single-sinker densimeter and measurements of the (p, ρ, T) relation of argon and nitrogen in the temperature range from (235 to 520) K at pressures up

- to 30 MPa. J Chem Thermodyn 1998;30(12):1571–88. https://doi.org/10.1006/jcht.1998.0421.
- [18] McLinden MO. Experimental techniques 1: direct methods. In: Wilhelm E, Letcher T, editors.
 Volume properties liquids, solutions and vapours. Cambridge: Royal Society of Chemistry; 2015.
 p. 73–99. https://doi.org/10.1039/9781782627043-00073.
- [19] Richter M, Kleinrahm R. Influence of adsorption and desorption on accurate density measurements of gas mixtures. J Chem Thermodyn 2014;74:58–66. https://doi.org/10.1016/j.jct.2014.03.020.
- [20] McLinden MO, Kleinrahm R, Wagner W. Force transmission errors in magnetic suspension densimeters. Int J Thermophys 2007;28(2):429–48. https://doi.org/10.1007/s10765-007-0176-0.
- [21] Bitter F. The magnetic susceptibilities of several organic gases. Phys Rev 1929;33(3):389–97. https://doi.org/10.1103/Phys.Rev.33.389.
- [22] Haynes WM (Ed.). CRC Handbook of Chemistry and Physics, 97th ed. Boca Raton: CRC Press; 2016.
- [23] May EF, Moldover MR, Schmidt JW. Electric and magnetic susceptibilities of gaseous oxygen:

 Present data and modern theory compared. Phys Rev A 2008;78:032522.

 https://doi.org/10.1103/PhysRevA.78.032522.
- [24] Minaev BF. Ab initio study of the ground state properties of molecular oxygen. Spectrochim Acta Part A 2004;60:1027–41. https://doi.org/10.1016/S1386-1425(03)00334-2.
- Hernández-Gómez R, Fernández-Vicente T, del Campo D, Val'ková M, Chytil M, Chamorro CR. [25] Characterization of a biomethane-like synthetic gas mixture through accurate density measurements pressures from (240)350) K and 14 MPa. Fuel 2017;206:420-8. to up to https://doi.org/10.1016/j.fuel.2017.06.040.
- [26] Hernández-Gómez R, Fernández-Vicente TE, Martín González MC, Mondéjar ME, Chamorro CR. Integration of biogas in the natural gas grid: thermodynamic characterization of a biogas-like mixture. J Chem Thermodyn 2015;84:60–6. https://doi.org/10.1016/j.jct.2014.12.028.
- [27] Mondéjar ME, Martín MC, Span R, Chamorro CR. New (*p*, *ρ*, *T*) data for carbon dioxide nitrogen mixtures from (250 to 400) K at pressures up to 20 MPa. J Chem Thermodyn 2011;43(12):1950–3. https://doi.org/10.1016/j.jct.2011.07.006.
- [28] Mondéjar ME, Villamañán RM, Span R, Chamorro CR. Accurate (p, ρ, T) data for two new (carbon

- dioxide + nitrogen) mixtures from (250 to 400) K at pressures up to 20 MPa. J Chem Thermodyn 2012;48:254–9. https://doi.org/10.1016/j.jct.2011.12.035.
- [29] Hernández-Gómez R, Tuma D, Segovia JJ, Chamorro CR. Experimental determination of (*p*, *ρ*, *T*) data for binary mixtures of methane and helium. J Chem Thermodyn 2016;96:1–11. https://doi.org/10.1016/j.jct.2015.12.006.
- [30] Hernández-Gómez R, Tuma D, Villamañán MA, Mondéjar ME, Chamorro CR. Accurate thermodynamic characterization of a synthetic coal mine methane mixture. J Chem Thermodyn 2014;68:253–59. https://doi.org/10.1016/j.jct.2013.09.023.
- [31] Hernández-Gómez R, Tuma D, Gómez-Hernández A, Chamorro CR. Accurate experimental (*p*, *ρ*, *T*) data for the introduction of hydrogen into the natural gas grid: thermodynamic characterization of the nitrogen–hydrogen binary system from 240 to 350 K and pressures up to 20 MPa. J Chem Eng Data 2017;62(12):4310–26. https://doi.org/10.1021/acs.jced.7b00694.
- [32] Hernández-Gómez R, Tuma D, Lozano-Martín D, Chamorro CR. Accurate experimental (*p*, *ρ*, *T*) data of natural gas mixtures for the assessment of reference equations of state when dealing with hydrogen-enriched natural gas. Int J Hydrogen Energy 2018;43(49):21983–98. https://doi.org/10.1016/j.ijhydene.2018.10.027.
- [33] Hernández-Gómez R, Tuma D, Pérez E, Chamorro CR. Accurate experimental (*p*, *ρ*, and *T*) data for the introduction of hydrogen into the natural gas grid (II): Thermodynamic characterization of the methane–hydrogen binary system from 240 to 350 K and pressures up to 20 MPa. J Chem Eng Data 2018;63(5):1613–30. https://doi.org/10.1021/acs.jced.7b01125.
- [34] Mondéjar ME, Fernández-Vicente TE, Haloua F, Chamorro CR. Experimental determination of (p, ρ, T) data for three mixtures of carbon dioxide with methane for the thermodynamic characterization of nonconventional energy gases. J Chem Eng Data 2012;57(9):2581–88. https://doi.org/10.1021/je300665n.
- [35] Mondéjar ME, Villamañán MA, Span R, Chamorro CR. (*p*, *ρ*, *T*) Behavior of two mixtures of carbon monoxide with nitrogen in the temperature range from (250 to 400) K and pressures up to 20 MPa. J Chem Eng Data 2011;56(10):3933–39. https://doi.org/10.1021/je2007764.
- [36] Span R, Lemmon EW, Jacobsen RT, Wagner W. A reference quality equation of state for nitrogen.

- Int J Thermophys 1998;19(4):1121–32. https://doi.org/10.1023/A:1022689625833.
- [37] JCGM 100. Evaluation of measurement data Guide to the expression of uncertainty in measurement (GUM). Joint committees for guides in Metrology. Sèvres, France: Bureau International des Poids et Mesures (BIPM); 2008.
- [38] Lemmon EW, Bell IH, Huber ML, McLinden MO. NIST standard reference database 23: reference fluid thermodynamic and transport properties-REFPROP, version 10.0. Gaithersburg MD: National Institute of Standards and Technology, Standard Reference Data Program; 2018.
- [39] Span R, Beckmüller R, Eckermann T, Herrig S, Hielscher S, Jäger A, Neumann T, Pohl S, Semrau B, Thol M. TREND. Thermodynamic Reference and Engineering Data 4.0. Bochum, Germany: Lehrstuhl für Thermodynamik, Ruhr-Universität Bochum; 2019.
- [40] Mantovani M, Chiesa P, Valenti G, Gatti M, Consonni S. Supercritical pressure—density–temperature measurements on CO₂–N₂, CO₂–O₂ and CO₂–Ar binary mixtures. J Supercrit Fluids 2011;61:34–43. https://doi.org/10.1016/j.supflu.2011.09.001.
- [41] Mazzoccoli M, Bosio B, Arato E. Pressure–density–temperature measurements of binary mixtures rich in CO₂ for pipeline transportation in the CCS process. J Chem Eng Data 2012;57(10):2774–83. https://doi.org/10.1021/je300590v.
- [42] Gururaja GJ, Tirunarayanan MA, Ramachandran A. Dynamic viscosity of gas mixtures. J Chem Eng Data 1967;12(4):562–7. https://doi.org/10.1021/je60035a024.
- [43] Al-Siyabi I. Effect of impurities on CO₂ stream properties. PhD Thesis, Edinburgh, Scotland: Heriot-Watt University; 2013.
- [44] Commodore JA, Deering CE, Marriott RA, Volumetric properties and phase behavior of sulfur dioxide, carbon disulfide and oxygen in high-pressure carbon dioxide fluid. Fluid Phase Equilib. 2018; 477:30-39. https://doi.org/10.1016/j.fluid.2018.08.012
- [45] Muirbrook NK. Experimental and thermodynamic study of the high-pressure vapor-liquid equilibria for the nitrogen-oxygen-carbon dioxide system. Ph.D. Thesis, Univ. Calif., Berkeley 1964.

Figures

Figure 1. p, T-phase diagram showing the experimental points measured (\bullet) and the calculated phase envelope (solid line) using the EOS-CG [6] for: (a) $(0.95 \text{ CO}_2 + 0.05 \text{ O}_2)$, (b) $(0.90 \text{ CO}_2 + 0.10 \text{ O}_2)$, and (c) $(0.80 \text{ CO}_2 + 0.20 \text{ O}_2)$ binary mixtures, respectively. The marked temperature and pressure ranges represent the range of the binary experimental data used for the development of the GERG-2008 [3] (blue dashed line), and the EOS-CG [6] (red dashed line), respectively, and the area of interest for the gas industry (black thin dashed line).

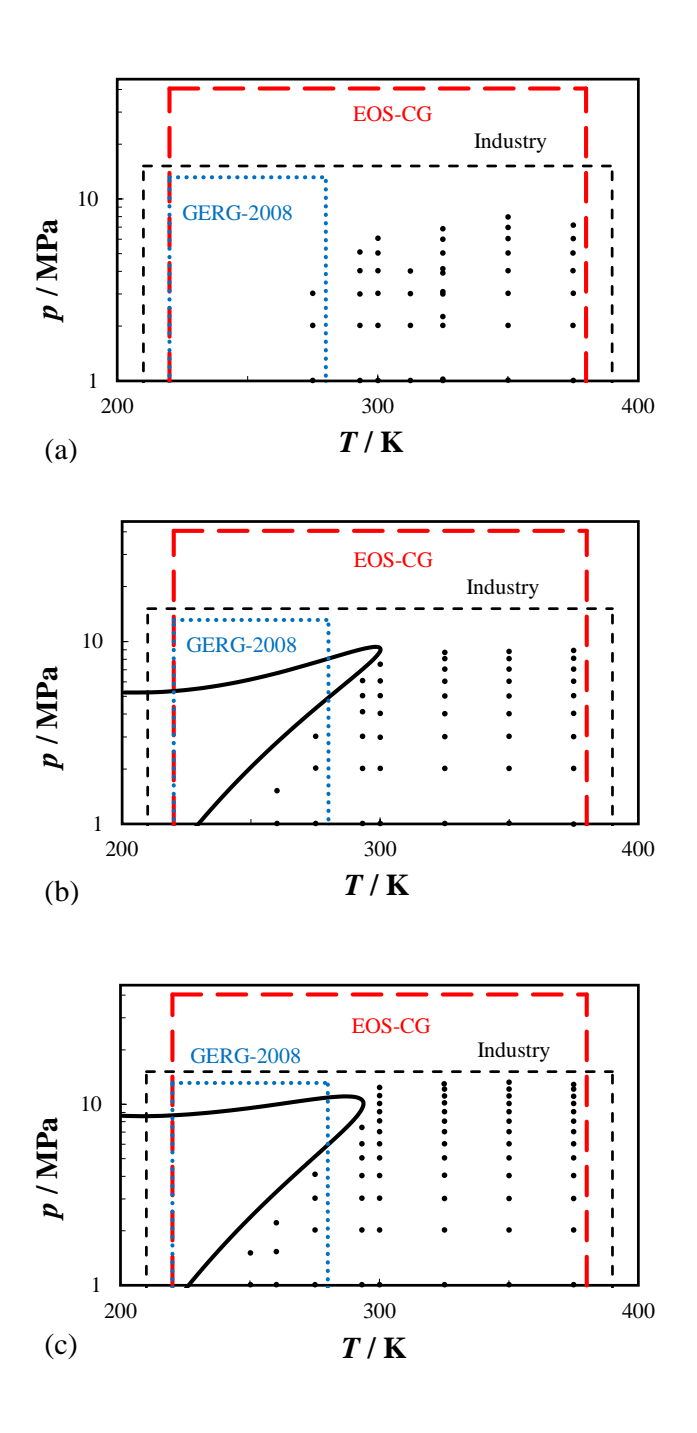


Figure 2. Relative deviations in density of experimental $(p, \rho_{\text{exp}}, T)$ data of the binary $(0.95 \text{ CO}_2 + 0.05 \text{ O}_2)$ mixture from density values calculated by the: (a) GERG-2008 [3], ρ_{GERG} , and (b) EOS-CG [6], ρ_{CG} , equations of state as a function of pressure for different temperatures: \triangle 275 K, \square 293.15 K, \bigcirc 300 K, \bigcirc 312.5 K, + 325 K, \times 350 K, \longrightarrow 375 K. Dashed lines indicate the expanded (k = 2) uncertainty of the corresponding EoS. Error bars on the 293.15 K data set indicate the expanded (k = 2) uncertainty of the experimental density.

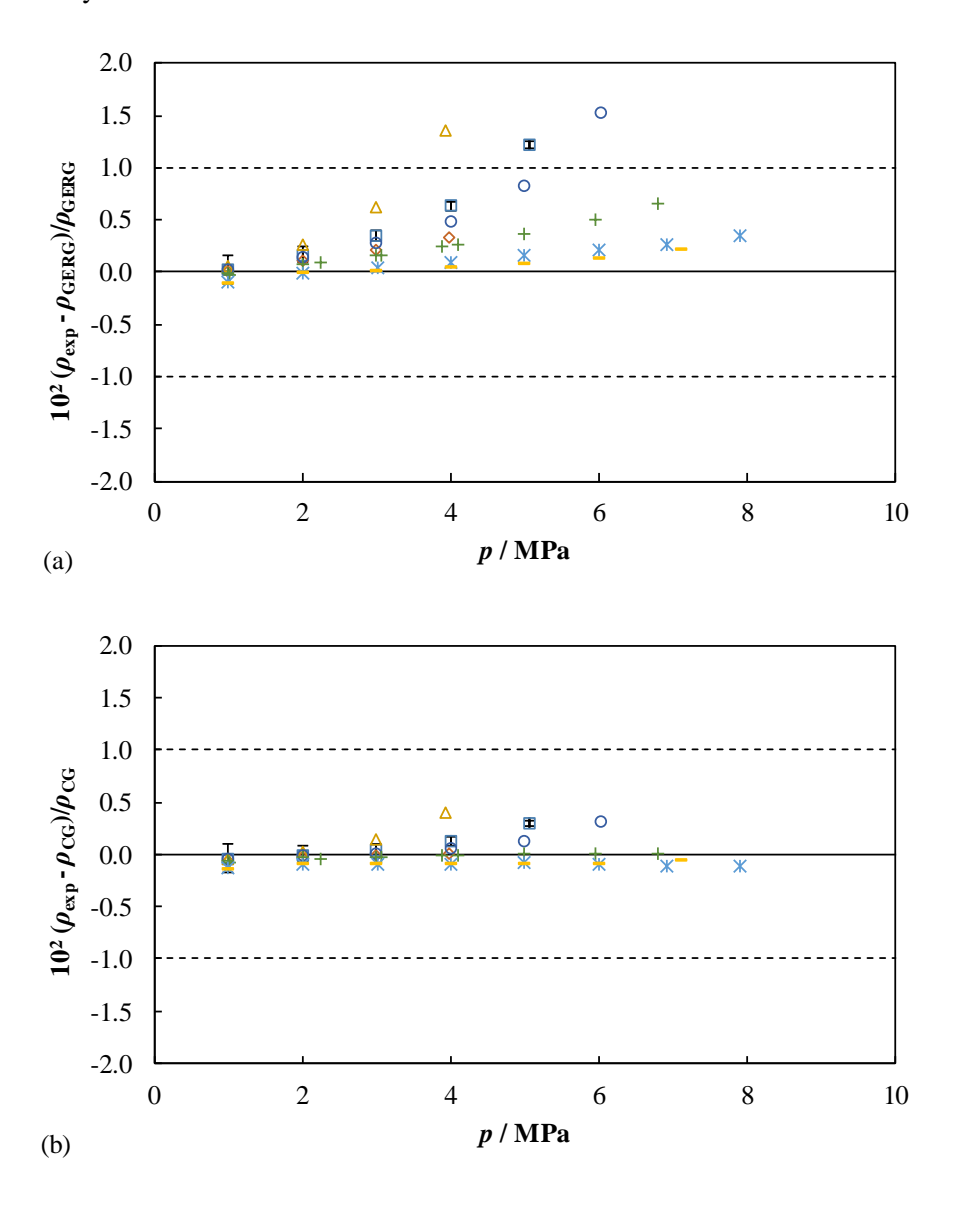


Figure 3. Relative deviations in density of experimental $(p, \rho_{\text{exp}}, T)$ data of the binary $(0.90 \text{ CO}_2 + 0.10 \text{ O}_2)$ mixture from density values calculated by the: (a) GERG-2008 [3], ρ_{GERG} , and (b) EOS-CG [6], ρ_{CG} , equations of state as a function of pressure for different temperatures: \diamondsuit 260 K, \times 275 K, \square 293.15 K, \bigcirc 300 K, + 325 K, \times 350 K, \longrightarrow 375 K. Dashed lines indicate the expanded (k = 2) uncertainty of the corresponding EoS. Error bars on the 293.15 K data set indicate the expanded (k = 2) uncertainty of the experimental density.

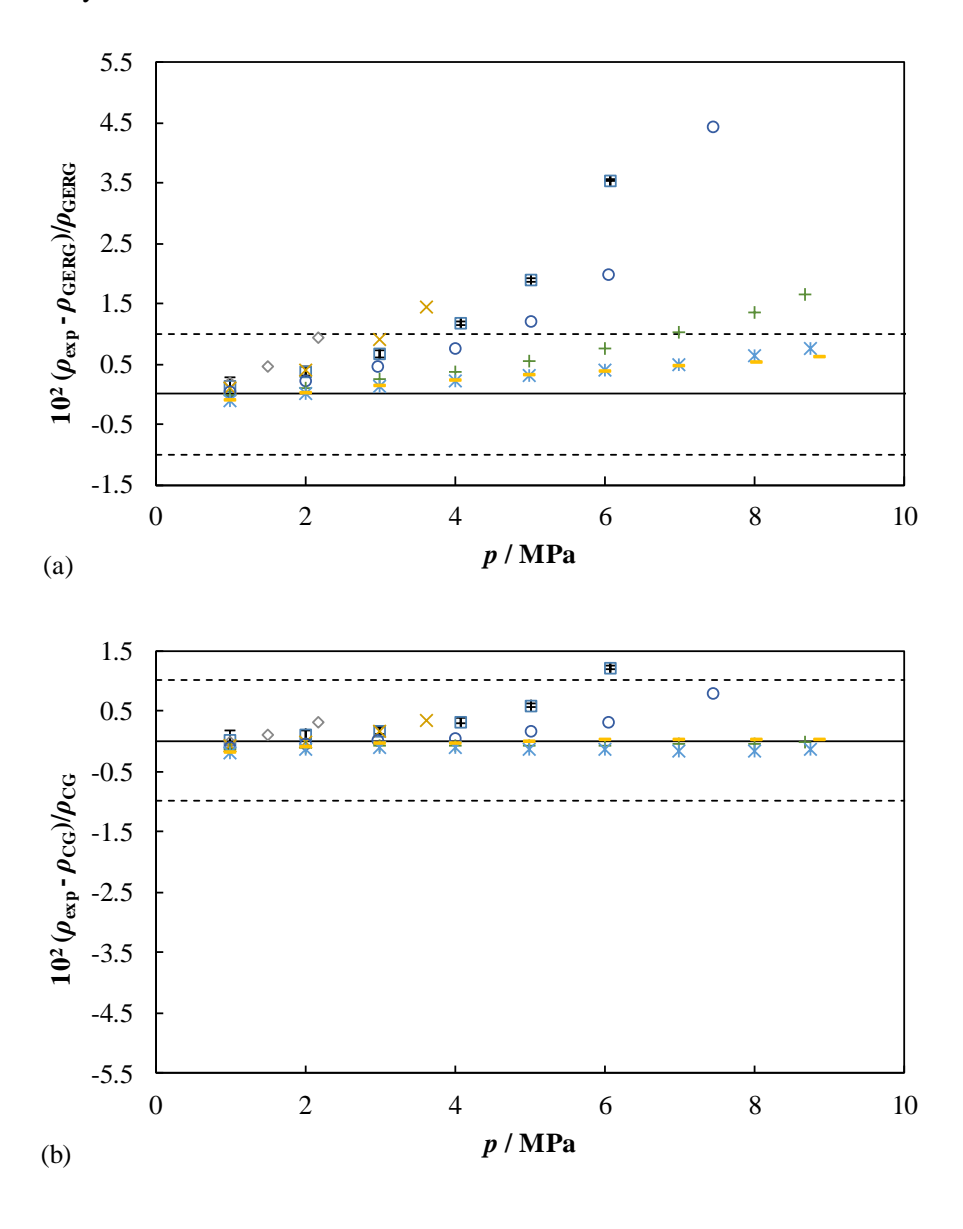
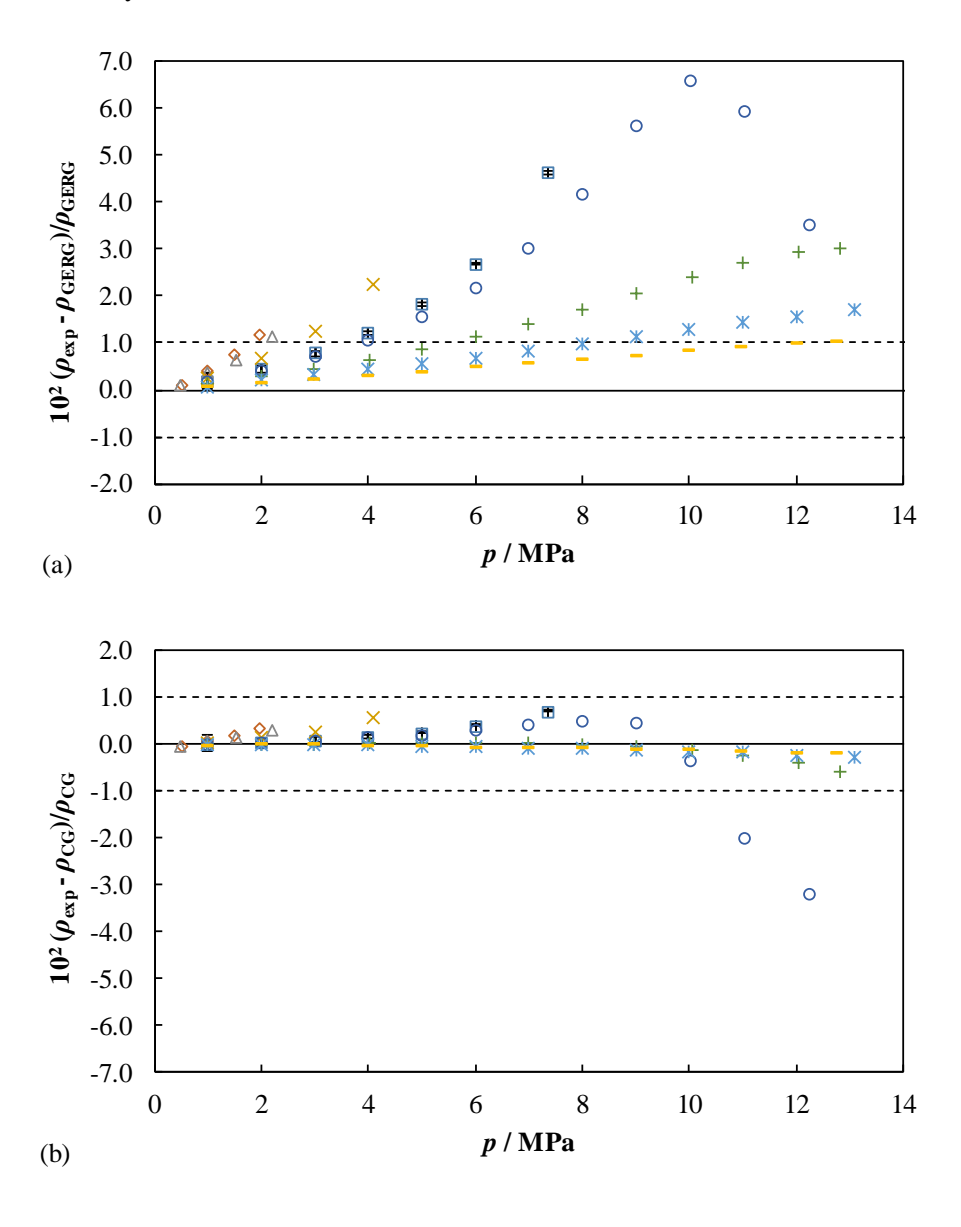


Figure 4. Relative deviations in density of experimental $(p, \rho_{\text{exp}}, T)$ data of the binary $(0.80 \text{ CO}_2 + 0.20 \text{ O}_2)$ mixture from density values calculated by the: (a) GERG-2008 [3], ρ_{GERG} , and (b) EOS-CG [6], ρ_{CG} , equations of state as a function of pressure for different temperatures: \diamondsuit 250 K, \triangle 260 K, \times 275 K, \square 293.15 K, \bigcirc 300 K, + 325 K, \times 350 K, \longrightarrow 375 K. Dashed lines indicate the expanded (k = 2) uncertainty of the corresponding EoS. Error bars on the 293.15 K data set indicate the expanded (k = 2) uncertainty of the experimental density.



Tables

Table 1. Purity, supplier, molar mass and critical parameters of the constituent components of the studied $(CO_2 + O_2)$ mixtures in this work.

	Purity / vol-%	Supplier A	<i>M</i> / g⋅mol ⁻¹	Critical parameters ^a		
	Turity / VOI-70	Supplier		<i>T</i> _c / K	p _c / MPa	
Carbon dioxide	99.9995	Air Liquide	44.010	304.13	7.3773	
Oxygen	99.9999	Linde	31.999	154.58	5.0430	

^a Critical parameters were obtained by using the default equation for each substance in REFPROP software [38].

Table 2. Composition with its expanded (k = 2) uncertainty of the studied binary ($CO_2 + O_2$) mixtures in this work. Impurity compounds are marked in *italics*.

	$(0.95 \text{ CO}_2 + 0.00 \text{ CO}$		$(0.90 \text{ CO}_2 + 0.10 \text{ O}_2)^{(b)}$		$(0.80 \text{ CO}_2 + 0.20 \text{ O}_2)^{(c)}$	
Component	$10^2 x_i /$	$10^2 U(x_i) /$	$10^2 x_i /$	$10^2 U(x_i) /$	$10^2 x_i /$	$10^2 U(x_i) /$
	mol/mol	mol/mol	mol/mol	mol/mol	mol/mol	mol/mol
Carbon dioxide	94.967781	0.001312	90.014271	0.001190	80.009178	0.001121
Oxygen	5.032082	0.001800	9.985591	0.001632	19.990681	0.001538
Argon	0.000005	0.000006	0.000010	0.000012	0.000020	0.000023
Nitrogen	0.000098	0.000110	0.000096	0.000105	0.000090	0.000094
Carbon monoxide	0.000029	0.000033	0.000028	0.000031	0.000026	0.000028
Propane	< 0.000001	< 0.000001	0.000001	0.000001	0.000001	0.000002
Nitric oxide	0.000004	0.000005	0.000004	0.000005	0.000004	0.000004
	impurities					
Carbon dioxide	94.967911	0.001312	90.014396	0.001190	80.009291	0.001121
Oxygen	5.032089	0.001800	9.985604	0.001632	19.990709	0.001538

⁽a) BAM cylinder no.: 1007-180626

⁽b) BAM cylinder no.: 1008-180626

⁽c) BAM cylinder no.: 9085-180116

Table 3. Results of the gas chromatographic (GC) analysis with its expanded (k = 2) uncertainty, and relative deviations between gravimetric preparation and GC analysis for the three (CO₂ + O₂) mixtures studied in this work. The results are followed by the gravimetric composition (non-normalized) of the validation mixtures employed.

	Concer	ntration	Relative deviation between gravimetric composition and GC analysis
Component	$10^2 x_i /$	$10^2 U(x_i) /$	%
	mol/mol	mol/mol	70
	$(0.95 \text{ CO}_2 + 0.0)$	05 O ₂) BAM cyl	linder no.: 1007-180626
Carbon dioxide	n. a.	n. a.	_
Oxygen	5.0054	0.0292	-0.530
Validatio	on mixture BAM	cylinder no.: 80	009-141027 (premixture of G 473)
Carbon dioxide	51.448818	0.000950	
Nitrogen	44.142855	0,001898	
Oxygen	4.408289	0.000340	
Argon	0.000009	0.000010	
Carbon monoxide	0.000018	0.000018	
Methane	0.000001	0.000001	
Hydrogen	0.000007	0.000006	
Nitric oxide	0.000002	0.000003	
Validatio	n mixture BAM	cylinder no.: 10	005-180528 (premixture of G 471)
Carbon dioxide	36.238235	0.000802	
Nitrogen	57.952277	0.001260	
Oxygen	5.809458	0.001102	
Argon	0.000006	0.000007	
Carbon monoxide	0.000014	0.000013	
Propane	< 0.000001	< 0.000001	
Hydrogen	0.000008	0.000009	
Nitric oxide	0.000002	0.000002	

(0.90 CO ₂ + 0.10 O ₂) BAM cylinder no.: 1008-180626						
Carbon dioxide	n. a.	n. a.	_			
Oxygen	9.9858	0.0036	0.002			
Va	llidation mixture	BAM cylinder	no.: 1028-190729 (G 033)			
Carbon dioxide	90.460031	0.001522				
Oxygen	9.539830	0.002090				
Argon	0.000010	0.000011				
Nitrogen	0.000095	0.000105				
Carbon monoxide	0.000028	0.000031				
Propane	0.000001	0.000001				
Nitric oxide	0.000005	0.000005				
Va	lidation mixture	BAM cylinder	no.: 1029-190729 (G 033)			
Carbon dioxide	89.489623	0.001524				
Oxygen	10.510238	0.002094				
Argon	0.000011	0.000012				
Nitrogen	0.000095	0.000104				
Carbon monoxide	0.000028	0.000031				
Propane	0.000001	0.000001				
Nitric oxide	0.000004	0.000005				
	$(0.80 \text{ CO}_2 + 0.20)$	0 O ₂) BAM cyl	inder no.: 9085-180116			
Carbon dioxide	n. a.	n. a.	_			
Oxygen	19.9924	0.0048	0.009			
Va	lidation mixture	BAM cylinder	no.: 9097-180205 (G 033)			
Carbon dioxide	81.017404	0.001269				
Oxygen	18.982455	0.001742				

0.000022

0.000019

Argon

Nitrogen	0.000091	0.000095
Carbon monoxide	0.000026	0.000028
Propane	0.000001	0.000002
Nitric oxide	0.000004	0.000004

Validation mixture BAM cylinder no.: 9099-180205 (G 033)

Carbon dioxide	79.011446	0.001265
Oxygen	20.988412	0.001737
Argon	0.000021	0.000025
Nitrogen	0.000090	0.000093
Carbon monoxide	0.000026	0.000027
Propane	0.000002	0.000002
Nitric oxide	0.000003	0.000004

Table 4. Contributions to the expanded (k = 2) overall uncertainty in density, $U_T(\rho_{exp})$, for the three (CO₂ + O₂) mixtures studied in this work.

Source	Contribution $(k = 2)$	Units	Estimation in density $(k = 2)$					
Source	Contribution (k = 2)	Omts	kg·m ⁻³	%				
$(0.95 \text{ CO}_2 + 0.05 \text{ O}_2)$								
Temperature, T	0.004	K	< 0.010	< 0.0058				
Pressure, p	< 0.004	MPa	(0.052 - 0.20)	(0.068 - 0.39)				
Composition, x_i	< 0.0004	mol·mol⁻¹	< 0.083	< 0.0076				
Density, ρ	(0.026 - 0.043)	$kg \cdot m^{-3}$	(0.026 - 0.043)	(0.026 - 0.18)				
Sum			(0.058 - 0.21)	(0.075 - 0.41)				
$(0.90 \text{ CO}_2 + 0.10 \text{ O}_2)$								
Temperature, T	0.004	K	< 0.020	< 0.0088				
Pressure, p	< 0.004	MPa	(0.051 - 0.30)	(0.057 - 0.98)				
Composition, x_i	< 0.0004	mol∙mol⁻¹	< 0.026	< 0.011				
Density, ρ	(0.027 - 0.052)	kg⋅m ⁻³	(0.027 - 0.052)	(0.022 - 0.19)				
Sum			(0.058 - 0.30)	(0.064 - 1.0)				
	(0.80	$CO_2 + 0.20 O_2$						
Temperature, T	0.004	K	< 0.049	< 0.012				
Pressure, p	< 0.005	MPa	(0.050 - 0.34)	(0.042 - 0.74)				
Composition, x_i	< 0.0004	mol·mol⁻¹	< 0.037	< 0.0082				
Density, ρ	(0.029 - 0.083)	kg⋅m ⁻³	(0.029 - 0.083)	(0.017 - 0.30)				
Sum			(0.057 - 0.35)	(0.049 - 0.80)				

Table 5. Experimental $(p, \rho_{\text{exp}}, T)$ measurements for the gaseous binary $(0.95 \text{ CO}_2 + 0.05 \text{ O}_2)$ mixture, absolute and relative expanded (k = 2) uncertainty in density, $U(\rho_{\text{exp}})$, and relative deviations from the density given by the GERG-2008 [3], ρ_{GERG} , and the EOS-CG [6], ρ_{CG} , equations of state. Normalized composition of the gaseous mixture is given in Table 2.

(147) (14D) (2)		$ ho_{ m exp}$ /	$U(ho_{ m exp})$ /	10^{2}	$10^2 (ho_{ m exp}$ -	$10^2 (\rho_{\rm exp} -$				
$T/K^{(a)}$	p / MPa ^(a)	kg⋅m ⁻³	kg⋅m ⁻³	$U(ho_{ m exp})/ ho_{ m exp}$	$ ho_{ m GERG})/ ho_{ m GERG}$	$ ho_{\mathrm{CG}})/ ho_{\mathrm{CG}}$				
	275 K isotherm									
275.001	3.940	109.732	0.037	0.034	1.35	0.41				
275.005	3.003	72.969	0.033	0.045	0.62	0.16				
275.001	1.999	43.849	0.029	0.067	0.26	0.04				
275.002	0.998	20.228	0.027	0.132	0.05	-0.03				
		25	93.15 K iso	therm						
293.100	5.066	133.334	0.039	0.030	1.22	0.30				
293.101	3.999	93.138	0.035	0.037	0.63	0.13				
293.098	2.983	63.642	0.032	0.050	0.34	0.05				
293.099	1.999	39.803	0.029	0.072	0.17	0.01				
293.094	0.999	18.728	0.026	0.141	0.03	-0.04				
			300 K isotl	nerm						
299.946	6.024	165.383	0.043	0.026	1.52	0.33				
299.946	5.001	121.053	0.038	0.031	0.82	0.14				
299.946	4.003	88.437	0.034	0.039	0.48	0.06				
299.945	3.000	61.548	0.031	0.051	0.28	0.02				
299.949	1.999	38.512	0.029	0.074	0.14	< 0.01				
299.949	0.999	18.226	0.026	0.145	0.02	-0.04				
		3	312.5 K isot	therm						
312.472	3.988	80.993	0.033	0.041	0.34	0.02				
312.476	2.987	57.253	0.031	0.054	0.21	< 0.01				
-						-				

312.475	2.001	36.462	0.028	0.078	0.11	-0.02			
312.474	0.999	17.385	0.026	0.151	0.01	-0.05			
325 K isotherm									
324.954	6.804	151.790	0.041	0.027	0.65	0.01			
324.954	5.950	125.498	0.038	0.031	0.50	0.02			
324.954	4.999	99.738	0.036	0.036	0.37	0.01			
324.953	4.102	78.087	0.033	0.042	0.27	< 0.01			
324.953	3.882	73.095	0.033	0.044	0.24	-0.01			
324.953	3.066	55.564	0.031	0.055	0.16	-0.02			
324.953	2.986	53.926	0.030	0.056	0.16	-0.01			
324.952	2.243	39.219	0.029	0.073	0.09	-0.03			
324.955	2.000	34.625	0.028	0.081	0.08	-0.02			
324.952	1.014	16.891	0.026	0.155	-0.03	-0.07			
324.953	0.997	16.594	0.026	0.157	-0.01	-0.06			
		3	350 K isot	herm					
349.938	7.897	153.813	0.042	0.027	0.35	-0.11			
349.939	6.910	129.216	0.039	0.030	0.26	-0.11			
349.939	6.001	108.351	0.036	0.034	0.22	-0.08			
349.937	4.999	87.007	0.034	0.039	0.16	-0.08			
349.938	3.999	67.238	0.032	0.047	0.10	-0.08			
349.937	3.005	48.906	0.030	0.061	0.04	-0.09			
349.937	1.999	31.537	0.028	0.088	-0.01	-0.09			
349.938	0.999	15.308	0.026	0.169	-0.09	-0.13			
		3	375 K isot	herm					
374.925	7.119	117.407	0.037	0.032	0.21	-0.05			
374.922	5.997	96.019	0.035	0.036	0.13	-0.08			
374.921	4.998	78.021	0.033	0.042	0.07	-0.10			

374.921	3.999	60.906	0.031	0.051	0.04	-0.09
374.923	2.999	44.608	0.029	0.065	0.01	-0.09
374.920	1.999	29.064	0.027	0.094	-0.02	-0.08
374.922	0.999	14.188	0.026	0.181	-0.11	-0.14

⁽a) Expanded uncertainties (k = 2): $U(p > 3)/\text{MPa} = 75 \cdot 10^{-6} \cdot \frac{p}{\text{MPa}} + 3.5 \cdot 10^{-3}$; $U(p < 3)/\text{MPa} = 60 \cdot 10^{-6} \cdot 10^{-6} \cdot 10^{-6} \cdot 10^{-6}$

$$10^{-6} \cdot \frac{p}{\text{MPa}} + 1.7 \cdot 10^{-3}; \ U(T) = 4 \text{ mK}; \\ \frac{U(\rho)}{\text{kg} \cdot \text{m}^{-3}} = 2.5 \cdot 10^4 \frac{\chi_{\text{S}}}{\text{m}^3 \cdot \text{kg}^{-1}} + 1.1 \cdot 10^{-4} \cdot \frac{\rho}{\text{kg} \cdot \text{m}^{-3}} + 2.3 \cdot 10^{-2}.$$

Table 6. Experimental $(p, \rho_{\text{exp}}, T)$ measurements for the gaseous binary $(0.90 \text{ CO}_2 + 0.10 \text{ O}_2)$ mixture, absolute and relative expanded (k = 2) uncertainty in density, $U(\rho_{\text{exp}})$, and relative deviations from the density given by the GERG-2008 [3], ρ_{GERG} , and the EOS-CG [6], ρ_{CG} , equations of state. Normalized composition of the gaseous mixture is given in Table 2.

T (X(0) (1) (0)		$ ho_{ m exp}$ /	$U(ho_{ m exp})$ /	10^{2}	$10^2 \left(ho_{ m exp} - ight.$	10^2 ($ ho_{ m exp}$ -			
$T/K^{(a)}$	p / MPa ^(a)	kg⋅m ⁻³	kg·m ⁻³	$U(ho_{ m exp})/ ho_{ m exp}$	$ ho_{ m GERG})/ ho_{ m GERG}$	$ ho_{\mathrm{CG}})/ ho_{\mathrm{CG}}$			
260 K isotherm									
260.020	2.184	52.302	0.032	0.061	0.93	0.33			
260.019	1.508	33.644	0.030	0.088	0.45	0.12			
260.017	0.998	21.279	0.028	0.133	0.18	-0.01			
			275 K isotł	nerm					
274.989	3.627	90.941	0.036	0.040	1.43	0.34			
274.984	2.999	70.068	0.034	0.048	0.90	0.17			
274.980	2.008	42.944	0.031	0.071	0.39	0.01			
274.976	0.998	19.835	0.028	0.141	0.09	-0.06			
		29	93.15 K iso	therm					
293.070	6.067	171.349	0.045	0.026	3.55	1.21			
293.066	5.010	123.409	0.040	0.032	1.90	0.60			
293.063	4.087	92.196	0.036	0.039	1.17	0.34			
293.065	3.004	62.381	0.033	0.052	0.67	0.18			
293.069	1.999	38.950	0.030	0.077	0.38	0.11			
293.069	0.999	18.430	0.028	0.150	0.14	0.02			
			300 K isotł	nerm					
299.924	7.455	231.402	0.052	0.022	4.43	0.81			
299.926	6.044	153.702	0.043	0.028	1.99	0.33			
299.925	5.017	115.524	0.039	0.033	1.22	0.17			
299.924	4.001	85.165	0.035	0.041	0.75	0.07			

299.924	2.968	59.083	0.032	0.055	0.46	0.03
299.923	1.999	37.687	0.030	0.079	0.22	-0.03
299.924	0.999	17.908	0.028	0.154	0.03	-0.08
		3	325 K isot	therm		
324.938	8.665	206.873	0.049	0.024	1.66	< 0.01
324.938	7.994	182.298	0.046	0.025	1.36	-0.03
324.938	7.002	150.100	0.042	0.028	1.03	-0.03
324.938	6.000	121.618	0.039	0.032	0.75	-0.05
324.937	5.000	96.328	0.036	0.038	0.54	-0.06
324.937	3.999	73.596	0.034	0.046	0.37	-0.06
324.937	2.986	52.660	0.031	0.059	0.24	-0.06
324.936	2.000	33.932	0.029	0.086	0.10	-0.08
324.937	0.999	16.347	0.027	0.166	-0.03	-0.11
		3	350 K isot	therm		
349.926	8.743	168.502	0.044	0.026	0.75	-0.13
349.925	7.991	149.760	0.042	0.028	0.63	-0.14
349.924	6.999	126.611	0.040	0.031	0.48	-0.15
349.923	6.006	105.053	0.037	0.035	0.39	-0.13
349.924	5.000	84.653	0.035	0.041	0.29	-0.11
349.925	3.999	65.634	0.033	0.050	0.21	-0.09
349.925	2.999	47.789	0.031	0.064	0.12	-0.10
349.925	2.001	30.997	0.029	0.093	0.02	-0.11
349.924	1.001	15.092	0.027	0.178	-0.10	-0.17
		3	375 K isot	therm		
374.915	8.878	148.273	0.042	0.028	0.60	0.01
374.915	8.034	131.519	0.040	0.030	0.53	0.02
374.913	6.993	111.704	0.038	0.034	0.45	0.01

374.913	6.009	93.842	0.036	0.038	0.38	0.02
374.912	5.001	76.325	0.034	0.044	0.29	< 0.01
374.912	4.001	59.713	0.032	0.053	0.21	-0.02
374.912	2.986	43.583	0.030	0.069	0.12	-0.05
374.912	1.999	28.563	0.028	0.099	0.02	-0.08
374.914	0.992	13.874	0.027	0.192	-0.12	-0.18

⁽a) Expanded uncertainties (k = 2): $U(p > 3)/\text{MPa} = 75 \cdot 10^{-6} \cdot \frac{p}{\text{MPa}} + 3.5 \cdot 10^{-3}$; $U(p < 3)/\text{MPa} = 60 \cdot 10^{-6} \cdot 10^{-6} \cdot 10^{-6} \cdot 10^{-6}$

$$10^{-6} \cdot \frac{p}{\text{MPa}} + 1.7 \cdot 10^{-3}; \ U(T) = 4 \text{ mK}; \\ \frac{U(\rho)}{\text{kg} \cdot \text{m}^{-3}} = 2.5 \cdot 10^4 \frac{\chi_{\text{S}}}{\text{m}^3 \cdot \text{kg}^{-1}} + 1.1 \cdot 10^{-4} \cdot \frac{\rho}{\text{kg} \cdot \text{m}^{-3}} + 2.3 \cdot 10^{-2}.$$

Table 7. Experimental $(p, \rho_{\text{exp}}, T)$ measurements for the gaseous binary $(0.80 \text{ CO}_2 + 0.20 \text{ O}_2)$ mixture, absolute and relative expanded (k = 2) uncertainty in density, $U(\rho_{\text{exp}})$, and relative deviations from the density given by the GERG-2008 [3], ρ_{GERG} , and the EOS-CG [6], ρ_{CG} , equations of state. Normalized composition of the gaseous mixture is given in Table 2.

T/ K ^(a) p / MPa ^(a) kg·m³ / kg·m³ $U(\rho_{exp})/\rho_{exp}$ $\rho_{GERG})/\rho_{GERG}$ $\rho_{CG})/\rho_{CG}$ 250.048 1.951 45.821 0.034 0.075 1.18 0.33 250.050 1.498 33.661 0.033 0.098 0.76 0.19 250.051 0.998 21.478 0.032 0.147 0.40 0.07 250.051 0.499 10.322 0.030 0.293 0.09 -0.06 260.034 2.197 49.467 0.035 0.070 1.12 0.30 260.034 0.998 20.468 0.031 0.153 0.35 0.07 260.034 0.497 9.843 0.030 0.305 0.09 -0.04 275 K isotherm 275.006 4.073 97.460 0.040 0.041 2.26 0.56 275.007 2.006 40.820 0.033 0.081 0.68 0.13	T / W(a) / MD-(a		$ ho_{ m exp}$ /	$U(ho_{ m exp})$	10^{2}	10^2 ($ ho_{ m exp}$ -	$10^2 (\rho_{\rm exp} - $	
250.048	$T / K^{(a)}$	•		$/ \text{ kg} \cdot \text{m}^{-3}$	$U(ho_{ m exp})/ ho_{ m exp}$	$ ho_{ m GERG}$)/ $ ho_{ m GERG}$	$ ho_{\mathrm{CG}})/ ho_{\mathrm{CG}}$	
250.050				250 K iso	therm			
250.051 0.998 21.478 0.032 0.147 0.40 0.07 250.051 0.499 10.322 0.030 0.293 0.09 -0.06 260 K isotherm 260.034 2.197 49.467 0.035 0.070 1.12 0.30 260.035 1.521 32.407 0.033 0.101 0.64 0.16 260.034 0.998 20.468 0.031 0.153 0.35 0.07 260.034 0.497 9.843 0.030 0.305 0.09 -0.04 275 K isotherm 275.006 4.073 97.460 0.040 0.041 2.26 0.56 275.008 2.999 65.416 0.036 0.055 1.25 0.27 275.007 2.006 40.820 0.033 0.081 0.68 0.13 275.006 0.999 19.153 0.031 0.161 0.27 0.03 293.092 7.364 201.810 0.051 0.025 4.63 0.70 293.092 6.001 143.794 0.045 0.031 2.68 0.39 293.093 5.000 110.844 0.041 0.037 1.82 0.24	250.048	1.951	45.821	0.034	0.075	1.18	0.33	
250.051 0.499 10.322 0.030 0.293 0.09 -0.06 260 K isotherm 260.034 2.197 49.467 0.035 0.070 1.12 0.30 260.035 1.521 32.407 0.033 0.101 0.64 0.16 260.034 0.998 20.468 0.031 0.153 0.35 0.07 260.034 0.497 9.843 0.030 0.305 0.09 -0.04 275 K isotherm 275.006 4.073 97.460 0.040 0.041 2.26 0.56 275.008 2.999 65.416 0.036 0.055 1.25 0.27 275.007 2.006 40.820 0.033 0.081 0.68 0.13 275.006 0.999 19.153 0.031 0.161 0.27 0.03 293.092 7.364 201.810 0.051 0.025 4.63 0.70 293.092 6.001 143.794 0.045 0.031 2.68 0.39 293.093 5.000 110.844 0.041 0.037 1.82 0.24	250.050	1.498	33.661	0.033	0.098	0.76	0.19	
260 K isotherm 260.034 2.197 49.467 0.035 0.070 1.12 0.30 260.035 1.521 32.407 0.033 0.101 0.64 0.16 260.034 0.998 20.468 0.031 0.153 0.35 0.07 260.034 0.497 9.843 0.030 0.305 0.09 -0.04 275 K isotherm 275.006 4.073 97.460 0.040 0.041 2.26 0.56 275.008 2.999 65.416 0.036 0.055 1.25 0.27 275.007 2.006 40.820 0.033 0.081 0.68 0.13 275.006 0.999 19.153 0.031 0.161 0.27 0.03 293.092 7.364 201.810 0.051 0.025 4.63 0.70 293.092 6.001 143.794 0.045 0.031 2.68 0.39 293.093 5.000 110.844 0.041 0.037 1.82 0.24	250.051	0.998	21.478	0.032	0.147	0.40	0.07	
260.034 2.197 49.467 0.035 0.070 1.12 0.30 260.035 1.521 32.407 0.033 0.101 0.64 0.16 260.034 0.998 20.468 0.031 0.153 0.35 0.07 260.034 0.497 9.843 0.030 0.305 0.09 -0.04 275.006 4.073 97.460 0.040 0.041 2.26 0.56 275.008 2.999 65.416 0.036 0.055 1.25 0.27 275.007 2.006 40.820 0.033 0.081 0.68 0.13 275.006 0.999 19.153 0.031 0.161 0.27 0.03 293.092 7.364 201.810 0.051 0.025 4.63 0.70 293.092 6.001 143.794 0.045 0.031 2.68 0.39 293.093 5.000 110.844 0.041 0.037 1.82 0.24	250.051	0.499	10.322	0.030	0.293	0.09	-0.06	
260.035 1.521 32.407 0.033 0.101 0.64 0.16 260.034 0.998 20.468 0.031 0.153 0.35 0.07 260.034 0.497 9.843 0.030 0.305 0.09 -0.04 275 K isotherm 275.006 4.073 97.460 0.040 0.041 2.26 0.56 275.008 2.999 65.416 0.036 0.055 1.25 0.27 275.007 2.006 40.820 0.033 0.081 0.68 0.13 275.006 0.999 19.153 0.031 0.161 0.27 0.03 293.092 7.364 201.810 0.051 0.025 4.63 0.70 293.092 6.001 143.794 0.045 0.031 2.68 0.39 293.093 5.000 110.844 0.041 0.037 1.82 0.24				260 K iso	therm			
260.034 0.998 20.468 0.031 0.153 0.35 0.07 260.034 0.497 9.843 0.030 0.305 0.09 -0.04 275 K isotherm 275.006 4.073 97.460 0.040 0.041 2.26 0.56 275.008 2.999 65.416 0.036 0.055 1.25 0.27 275.007 2.006 40.820 0.033 0.081 0.68 0.13 275.006 0.999 19.153 0.031 0.161 0.27 0.03 293.092 7.364 201.810 0.051 0.025 4.63 0.70 293.092 6.001 143.794 0.045 0.031 2.68 0.39 293.093 5.000 110.844 0.041 0.037 1.82 0.24	260.034	2.197	49.467	0.035	0.070	1.12	0.30	
260.034	260.035	1.521	32.407	0.033	0.101	0.64	0.16	
275 K isotherm 275.006 4.073 97.460 0.040 0.041 2.26 0.56 275.008 2.999 65.416 0.036 0.055 1.25 0.27 275.007 2.006 40.820 0.033 0.081 0.68 0.13 275.006 0.999 19.153 0.031 0.161 0.27 0.03 293.092 7.364 201.810 0.051 0.025 4.63 0.70 293.092 6.001 143.794 0.045 0.031 2.68 0.39 293.093 5.000 110.844 0.041 0.037 1.82 0.24	260.034	0.998	20.468	0.031	0.153	0.35	0.07	
275.006 4.073 97.460 0.040 0.041 2.26 0.56 275.008 2.999 65.416 0.036 0.055 1.25 0.27 275.007 2.006 40.820 0.033 0.081 0.68 0.13 275.006 0.999 19.153 0.031 0.161 0.27 0.03 293.092 7.364 201.810 0.051 0.025 4.63 0.70 293.092 6.001 143.794 0.045 0.031 2.68 0.39 293.093 5.000 110.844 0.041 0.037 1.82 0.24	260.034	0.497	9.843	0.030	0.305	0.09	-0.04	
275.008 2.999 65.416 0.036 0.055 1.25 0.27 275.007 2.006 40.820 0.033 0.081 0.68 0.13 275.006 0.999 19.153 0.031 0.161 0.27 0.03 293.15 K isotherm 293.092 7.364 201.810 0.051 0.025 4.63 0.70 293.092 6.001 143.794 0.045 0.031 2.68 0.39 293.093 5.000 110.844 0.041 0.037 1.82 0.24				275 K iso	therm			
275.007 2.006 40.820 0.033 0.081 0.68 0.13 275.006 0.999 19.153 0.031 0.161 0.27 0.03 293.15 K isotherm 293.092 7.364 201.810 0.051 0.025 4.63 0.70 293.092 6.001 143.794 0.045 0.031 2.68 0.39 293.093 5.000 110.844 0.041 0.037 1.82 0.24	275.006	4.073	97.460	0.040	0.041	2.26	0.56	
275.006 0.999 19.153 0.031 0.161 0.27 0.03 293.15 K isotherm 293.092 7.364 201.810 0.051 0.025 4.63 0.70 293.092 6.001 143.794 0.045 0.031 2.68 0.39 293.093 5.000 110.844 0.041 0.037 1.82 0.24	275.008	2.999	65.416	0.036	0.055	1.25	0.27	
293.092 7.364 201.810 0.051 0.025 4.63 0.70 293.092 6.001 143.794 0.045 0.031 2.68 0.39 293.093 5.000 110.844 0.041 0.037 1.82 0.24	275.007	2.006	40.820	0.033	0.081	0.68	0.13	
293.092 7.364 201.810 0.051 0.025 4.63 0.70 293.092 6.001 143.794 0.045 0.031 2.68 0.39 293.093 5.000 110.844 0.041 0.037 1.82 0.24	275.006	0.999	19.153	0.031	0.161	0.27	0.03	
293.092 6.001 143.794 0.045 0.031 2.68 0.39 293.093 5.000 110.844 0.041 0.037 1.82 0.24			2	93.15 K is	sotherm			
293.093 5.000 110.844 0.041 0.037 1.82 0.24	293.092	7.364	201.810	0.051	0.025	4.63	0.70	
	293.092	6.001	143.794	0.045	0.031	2.68	0.39	
293.092 4.000 82.990 0.038 0.045 1.22 0.14	293.093	5.000	110.844	0.041	0.037	1.82	0.24	
	293.092	4.000	82.990	0.038	0.045	1.22	0.14	
293.093 3.000 58.771 0.035 0.059 0.78 0.08	293.093	3.000	58.771	0.035	0.059	0.78	0.08	

293.093	2.000	37.241	0.032	0.087	0.44	0.03
293.091	0.999	17.779	0.030	0.170	0.18	< 0.01
			300 K iso	otherm		
299.946	12.259	478.560	0.083	0.017	3.50	-3.21
299.948	11.048	399.019	0.074	0.018	5.93	-2.02
299.946	10.015	326.890	0.065	0.020	6.57	-0.36
299.943	9.023	264.364	0.058	0.022	5.61	0.44
299.948	8.003	211.441	0.052	0.025	4.16	0.50
299.947	7.002	169.526	0.047	0.028	3.01	0.40
299.947	6.001	134.844	0.043	0.032	2.16	0.29
299.949	5.000	105.303	0.040	0.038	1.54	0.20
299.948	4.000	79.581	0.037	0.047	1.07	0.13
299.948	2.999	56.716	0.035	0.061	0.70	0.08
299.949	1.999	36.107	0.032	0.089	0.41	0.04
299.951	0.999	17.308	0.030	0.174	0.17	< 0.01
			325 K iso	otherm		
324.954	12.831	325.969	0.065	0.020	3.00	-0.56
324.955	12.035	295.650	0.061	0.021	2.93	-0.40
324.955	11.000	257.843	0.057	0.022	2.71	-0.23
324.955	10.066	225.884	0.053	0.024	2.41	-0.12
324.955	9.022	192.910	0.050	0.026	2.07	-0.03
324.955	8.000	163.394	0.046	0.028	1.71	< 0.01
324.955	7.000	136.975	0.043	0.032	1.40	0.02
324.956	6.000	112.754	0.041	0.036	1.11	0.02
324.956	5.000	90.434	0.038	0.042	0.86	0.02
324.956	4.009	69.968	0.036	0.051	0.64	0.01
324.956	2.989	50.395	0.033	0.066	0.45	0.01

	0.28	< 0.01
324.956 0.999 15.825 0.030 0.187	0.13	< 0.01
350 K isotherm		
349.939 13.100 260.198 0.057 0.022	1.70	-0.28
349.940 11.999 231.912 0.054 0.023	1.57	-0.23
349.938 10.996 207.061 0.051 0.025	1.44	-0.18
349.939 9.998 183.318 0.048 0.026	1.28	-0.15
349.939 8.999 160.609 0.046 0.028	1.13	-0.12
349.939 7.998 138.940 0.043 0.031	0.97	-0.09
349.939 6.999 118.408 0.041 0.035	0.83	-0.07
349.939 6.000 98.915 0.039 0.039	0.69	-0.05
349.939 4.999 80.345 0.037 0.045	0.56	-0.03
349.939 4.000 62.704 0.035 0.055	0.44	-0.02
349.939 2.991 45.765 0.033 0.071	0.32	< 0.01
349.938 2.004 29.964 0.031 0.103	0.21	< 0.01
349.937 0.999 14.599 0.029 0.199	0.08	-0.02
375 K isotherm		
374.925 12.757 212.673 0.051 0.024	1.03	-0.20
374.923 12.025 198.134 0.050 0.025	0.98	-0.19
374.923 10.978 177.772 0.047 0.027	0.90	-0.16
374.923 9.988 159.011 0.045 0.028	0.82	-0.14
374.922 8.996 140.736 0.043 0.031	0.73	-0.12
374.924 7.998 122.913 0.041 0.033	0.64	-0.10
374.923 6.999 105.643 0.039 0.037	0.55	-0.08
374.922 5.999 88.925 0.037 0.042	0.47	-0.07
374.924 5.005 72.873 0.035 0.049	0.38	-0.05
374.923 4.000 57.212 0.034 0.059	0.31	-0.03

374.923	2.986	41.958	0.032	0.076	0.23	-0.02
374.922	1.999	27.603	0.030	0.110	0.14	-0.02
374.922	0.999	13.550	0.029	0.211	0.04	-0.04

⁽a) Expanded uncertainties (k = 2): $U(p > 3)/\text{MPa} = 75 \cdot 10^{-6} \cdot \frac{p}{\text{MPa}} + 3.5 \cdot 10^{-3}$; $U(p < 3)/\text{MPa} = 60 \cdot 10^{-6} \cdot 10^{-6} \cdot 10^{-6} \cdot 10^{-6}$

$$10^{-6} \cdot \frac{p}{\text{MPa}} + 1.7 \cdot 10^{-3}; \ U(T) = 4 \text{ mK}; \\ \frac{U(\rho)}{\text{kg·m}^{-3}} = 2.5 \cdot 10^4 \frac{\chi_{\text{S}}}{\text{m}^3 \cdot \text{kg}^{-1}} + 1.1 \cdot 10^{-4} \cdot \frac{\rho}{\text{kg·m}^{-3}} + 2.3 \cdot 10^{-2}.$$

Table 8. Statistical analysis of the (p, ρ, T) data set processed with the GERG-2008 [3] and EOS-CG [6] for the three $(CO_2 + O_2)$ mixtures studied in this work, including literature data for comparable mixtures. AAD = absolute average deviation, Bias = average deviation, RMS = root mean square deviation, MaxD = maximum deviation.

			Covered	ranges	Experimental vs GERG-2008				Experimental vs EOS-CG			
Reference ^(a)	$x(O_2)$	$N^{(b)}$	<i>T</i> / K	<i>p</i> /	AAD	Bias	RMS	MaxD	AAD /	Bias / %	RMS	MaxD
			1 / K	MPa	/ %	/ %	/ %	/ %	%	Dias / /0	/ %	/ %
This work	0.050321	45	275-375	0.5-8	0.29	0.28	0.45	1.5	0.077	-0.0022	0.11	0.41
This work	0.099856	47	260-375	0.5-9	0.69	0.68	1.1	4.4	0.15	0.054	0.26	1.2
This work	0.199907	70	250-375	0.5-13	1.3	1.3	1.9	6.6	0.22	-0.052	0.50	3.2
Gururaja et al.	0.0.1.0	9	297-303	0.1	1.8	-1.7	3.3	7.6	1.8	-1.7	3.3	7.6
[42]	0.0-1.0	9	291-303	0.1	1.0	-1./	3.3	7.0	1.0	-1./	3.3	7.0
Mantovanni et	0.060700	96	303-383	1-20	1.4	-1.4	2.0	8.3	2.1	-2.1	2.8	13
al. [40] ^(c)	0.000700		202 202	1 20	1	1	2.0	0.5	2.1	2.1	2.0	15
Mantovanni et	0.129100	100	303-383	1-20	2.2	-2.2	2.8	13	3.5	-3.5	4.1	13
al. [40] ^(c)												
Mazzoccoli et	0.044200	12	273-293	1-7	2.4	2.4	2.9	6.7	1.8	1.8	2.5	6.6
al. [41]												

Mazzoccoli et	0.140000	10	272 202	1.7	1.2	0.4	1.0	5.0	1.0	0.80	2.5	7.2
al. [41]	0.148800	18	273-293	1-7	1.2	0.4	1.8	5.2	1.9	-0.89	2.5	7.2
Al-Siyabi [43]	0.050000	26	323-423	8-40	1.3	-1.1	1.5	3.0	1.5	-1.5	1.7	3.2
Commodore et	0.01246	112	324-400	2-35	0.17	0.09	0.26	1.2	0.15	0.0033	0.23	1.2
al. [44]	0.01240	112	324-400	2-33	0.17	4	0.20	1.2	0.13	0.0055	0.23	1.2
Muirbrook	0.035-0.4	32	273.15	Saturat	43	38	75	247	39	34	70	235
[45]	0.033-0.4	32	273.13	ion	43	50	13	<i>2</i> 4 7	39	54	70	233

^(a) Only measurements in the vapor and supercritical phase have been considered.

⁽b) Number of experimental points.

⁽c) Used for the EOS-CG development.